THE JOURNAL OF BIOLOGICAL CHEMISTRY Vol. 280, No. 27, Issue of July 8, pp. 25629–25636, 2005

Printed in U.S.A.

Mitochondrial Glycerol-3-phosphate Acyltransferase-1 Is Essential in Liver for the Metabolism of Excess Acyl-CoAs*

Received for publication, March 23, 2005, and in revised form, April 26, 2005
Published, JBC Papers in Press, May 6, 2005, DOI 10.1074/jbc.M503181200

Linda E. Hammond‡, Susanne Neschen§¶, Anthony J. Romanelli§, Gary W. Cline§, Olga R. Ilkayeva‖, Gerald I. Shulman§¶, Deborah M. Muoio‖, and Rosalind A. Coleman‡ ‡‡**

From the ‡Department of Nutrition, University of North Carolina, North Chapel Hill, Carolina 27599, the §Department of Internal Medicine and ¶Howard Hughes Medical Institute, Yale University School of Medicine, New Haven, Connecticut 06510, and the ‖Departments of Medicine and Pharmacology and Cancer Biology, Sarah W. Stedman Nutrition and Metabolism Center, Duke University, Durham, North Carolina 27710

***In vitro* studies suggest that the mitochondrial glycerol-3-phosphate acyltransferase-1 (mtGPAT1) isoform catalyzes the initial and rate-controlling step in glycerolipid synthesis and aids in partitioning acyl-CoAs toward triacylglycerol synthesis and away from degradative pathways. To determine whether the absence of mtGPAT1 would increase oxidation of acyl-CoAs and restrict the development of hepatic steatosis, we fed wild type and mtGPAT1$^{-/-}$ mice a diet high in fat and sucrose (HH) for 4 months to induce the development of obesity and a fatty liver. Control mice were fed a diet low in fat and sucrose (LL). With the HH diet, absence of mtGPAT1 resulted in increased partitioning of acyl-CoAs toward oxidative pathways, demonstrated by 60% lower hepatic triacylglycerol content and 2-fold increases in plasma β-hydroxybutyrate, acylcarnitines, and hepatic mRNA expression of mitochondrial HMG-CoA synthase. Despite the increase in fatty acid oxidation, liver acyl-CoA levels were 3-fold higher in the mtGPAT1$^{-/-}$ mice fed both diets. A lack of difference in CPT1 and FAS mRNA expression between genotypes suggested that the increased acyl-CoA content was not because of increased *de novo* synthesis, but instead, to an impaired ability to use long-chain acyl-CoAs derived from the diet, even when the dietary fat content was low. Hyperinsulinemia and reduced glucose tolerance on the HH diet was greater in the mtGPAT1$^{-/-}$ mice, which did not suppress the expression of the gluconeogenic genes glucose-6-phosphatase and phosphoenolpyruvate carboxykinase. This study demonstrates that mtGPAT1 is essential for normal acyl-CoA metabolism, and that the absence of hepatic mtGPAT1 results in the partitioning of fatty acids away from triacylglycerol synthesis and toward oxidation and ketogenesis.**

Hepatic steatosis, a feature of the metabolic syndrome, is a precursor for hepatosteatitis, cirrhosis, and liver failure (1). The initial and rate-controlling step in triacylglycerol synthesis is catalyzed by glycerol-3-phosphate acyltransferase (GPAT),[1] which uses long-chain acyl-CoAs to acylate glycerol 3-phosphate (2). Three GPAT activities have been identified in mammalian tissues, one in the endoplasmic reticulum (microsomal GPAT), and two in the mitochondria, mtGPAT1 and mtGPAT2 (2, 3). Although the independent roles of the three GPAT isoforms have not been established, the mtGPAT1 appears to be an important contributor to triacylglycerol synthesis. For example, mtGPAT1 activity and mRNA expression are up-regulated nutritionally and hormonally when excess calories are available from either dietary fat or carbohydrate (4–6). Conversely, mice that lack mtGPAT1 have a lower hepatic content of triacylglycerol and a lower rate of very low density lipoprotein secretion compared with wild type mice (7).

Directing acyl-CoAs toward either oxidative or synthetic pathways is key in the regulation of cellular energy metabolism and triacylglycerol accumulation. Both mtGPAT1 and carnitine palmitoyltransferase-1, the rate-limiting step for β-oxidation, are intrinsic enzymes of the outer mitochondrial membrane where their reciprocal regulation by AMP-activated protein kinase (AMPK) would allow them to play coordinated roles in directing the fate of acyl-CoAs. *In vitro* studies show that AMPK phosphorylates acetyl-CoA carboxylase, thereby decreasing the product of acetyl-CoA carboxylase, malonyl-CoA, the allosteric inhibitor of carnitine palmitoyltransferase-1 (8). Concomitantly, AMPK inhibits mtGPAT1, decreasing the entry of acyl-CoAs into the pathway of glycerolipid synthesis (9–11).

When fed diets high in fat and sucrose C57BL/6J mice develop severe obesity, hyperglycemia, and hyperinsulinemia (12), and hepatic mtGPAT1 specific activity increases 2-fold (13). Overexpression of mtGPAT1 in rat hepatocytes increases both triacylglycerol mass and the incorporation of [^{14}C]oleate into triacylglycerol, while decreasing [^{14}C]oleate incorporation into oxidation products (13, 14). Thus, because the mitochondrial isoform of GPAT comprises 30–50% of total hepatic GPAT activity, we reasoned that the absence of mtGPAT1 would divert excess hepatic acyl-CoAs toward

* This work was supported in part by Grants DK56598 (to R. A. C.), F31 GM20920 (to L. E. H.), K01 DK67200 (to D. M. M.), and DK40936 (to G. I. S.), P30 DK45735 (to G. I. S.), U24 DK59635 (to G. I. S.), and DK56350 to the University of North Carolina, CNRU. The costs of publication of this article were defrayed in part by the payment of page charges. This article must therefore be hereby marked "*advertisement*" in accordance with 18 U.S.C. Section 1734 solely to indicate this fact.

** Recipient of a Distinguished Clinical Scientist Award from the American Diabetes Association and an Investigator of the Howard Hughes Medical Institute.

‡‡ To whom correspondence should be addressed: Dept. of Nutrition, 2301 Hooker Research Bldg., University of North Carolina, Chapel Hill, NC 27599. Tel.: 919-966-7213; Fax: 919-966-7216; E-mail: rcoleman@unc.edu.

[1] The abbreviations used are: GPAT, glycerol-3-phosphate acyltransferase; ACO, acyl-CoA oxidase; AMPK, AMP-activated kinase; HH, high fat/high sucrose; LL, low fat/low sucrose; mtGPAT, mitochondrial GPAT; mtHS2, mitochondrial 3-hydroxy-3-methylglutaryl-CoA synthase; PEPCK, phosphoenolpyruvate carboxykinase; PPAR, peroxisome proliferator activated receptor; SREBP, sterol regulatory element binding protein; FAS, fatty acid synthase; SCD, stearoyl-CoA desaturase; ANOVA, analysis of variance; HMG, hydroxymethylglutaryl; LC/MS/MS, high performance liquid chromatography/mass spectrometry/mass spectrometry.

β-oxidation, even when mice are fed a diet designed to promote obesity and hepatic steatosis.

MATERIALS AND METHODS

Animals and Diets—Animal protocols were approved by the University of North Carolina at Chapel Hill Institutional Animal Care and Use Committee. Generation of mtGPAT1$^{-/-}$ mice was previously described (7). F1 mice were crossed six times with C57BL/6J mice to transfer the null mtGPAT1 mutation onto a C57BL/6J genetic background (>99%). Heterozygotes were then intercrossed to obtain mtGPAT1 wild type, heterozygous, and homozygous knock-out mtGPAT1 mice. Because the male and female mtGPAT1$^{-/-}$ mice had similar phenotypes, unless otherwise noted, only data from males are shown. Mice were housed in a pathogen-free barrier facility on a 12-h light/dark cycle and had free access to water and food. Weaned mice were fed Prolab RMH 3000 SP76 chow (26.0% kcal protein, 14% kcal fat, and 60% kcal carbohydrate). From ages 2 to 6 months they were fed either a high fat/high sucrose (HH) diet that results in marked lipogenesis, triacylglycerol synthesis, hyperlipidemia, obesity, and insulin resistance (12, 15–17) or the complementary low fat/low sucrose (LL) diet (12). The high sucrose content of the diet promotes hepatic lipogenesis by increasing insulin secretion and activation of SREBP1c and by by-passing the rate-limiting step of glycolysis, phosphofructokinase, thereby increasing the production of glycerol 3-phosphate (18). The diets were LL: Research Diet D12328 (16.4% kcal protein, 73.1% kcal carbohydrate (611 g/kg corn starch, 124 g/kg maltodextrin 10), 10.5% kcal fat (29.3 g/kg coconut oil, 18.3 g/kg soybean oil)) and HH: Research Diet D12331 (16.4% kcal protein, 25.5% kcal carbohydrate (175 g/kg sucrose, 170 g/kg maltodextrin 10), 58% kcal fat (333.5 g/kg coconut oil, 25 g/kg soybean oil)).

Blood Chemistries and Lipids—Mice were fasted for 4–6 h before blood collection. Plasma triacylglycerol (triglyceride, Stanbio, Boerne, TX), total cholesterol (cholesterol CII, Wako Diagnostics, Richmond, VA), free fatty acids (NEFA, Wako Diagnostics, Richmond, VA), glucose (glucose CII, Wako Diagnostics), and β-hydroxybutyrate (Wako Diagnostics) were determined by enzymatic colorimetric methods. Insulin (ultrasensitive rat insulin enzyme-linked immunosorbent assay, Crystal Chemical, Chicago, IL) and leptin (mouse leptin enzyme-linked immunosorbent assay, Crystal Chemical) were determined by enzyme-linked immunosorbent assay. For the glucose tolerance test, mice were injected intraperitoneally with 1 mg of glucose/g body weight. Plasma was collected at time 0, and at 15, 30, 60, 90, and 120 min after the glucose injection. To calculate the insulin resistance index, the areas under the glucose and insulin curves in the glucose tolerance test were calculated by multiplying the cumulative mean height of the glucose values (1 mg/ml = 1 cm) and the insulin values (1 ng/ml = 1 cm) by time (60 min = 1 cm) (19). The insulin resistance index is the product of the areas under the glucose and the insulin curves.

Liver Triacylglycerol and Lysophosphatidic Content—Liver was homogenized in 10 mM Tris, pH 7.4, 250 mM sucrose, 1 mM dithiothreitol, and 1 mM EDTA. Lipids were extracted from the homogenate with chloroform/methanol (2/1, v/v) (20). For triacylglycerol measurements, total lipid extracts were dried under N_2 gas, resuspended in isopropyl alcohol, 1% Triton X-100 and analyzed colorimetrically as described above. To measure lysophosphatidic acid content, ~100 mg of liver was homogenized in chloroform/methanol (1:1, v/v) with 1 nM C17-lysophosphatidic acid internal standard. After phase separation with distilled H_2O, samples were homogenized and centrifuged, and the methanol/water phase was collected. The supernatant was applied to conditioned Waters Oasis MAX extraction cartridges (Waters Corp., Milford, MA) and after a washing step, lysophosphatidic acid was eluted using methanol. Individual lysophosphatidic acid derivatives were measured using LC/MS/MS analysis. Total lysophosphatidic acid content was expressed as the sum of individual species.

Liver Fatty Acyl-CoA Content—For solid-phase extraction of medium, long-chain, and very long-chain fatty acyl-CoAs (21), ~100 mg of liver together with a C17:0 acyl-CoA-ester internal standard was homogenized on ice in 50 mM KH_2PO_4, 50% 2-propanol. An equal volume of acetonitrile and 1/32 of the final volume of $(NH_4)_2SO_4$ was added, the emulsion was vortexed, and the supernatant was separated by centrifugation. The supernatant was diluted with 100 mM KH_2PO_4 and purified using Oligonucleotide Purification Cartridges (Applied Biosystems, Foster City, CA). Following a drying step, fatty acyl-CoA fractions were dissolved in methanol/H_2O (1:1, v/v) and subjected to LC/MS/MS analysis. A turbo ion spray source was interfaced with an API 3000 tandem mass spectrometer (Applied Biosystems, Foster City, CA) in conjunction with two PerkinElmer 200 Series micro pumps and a 200 Series autosampler (PerkinElmer Life Sciences). The transition pairs $[M\text{-}2H]^{2-}$:$[M\text{-}H\text{-}80]^{-}$ (Q1 and Q3) were monitored in −MRM (multiple reaction monitoring) mode for each fatty acyl-CoA metabolite. Total fatty acyl-CoA content is expressed as the sum of individual species.

Liver Acylcarnitine Content—Liver specimens (~75 mg) were homogenized in 9 volumes of de-ionized water using a Potter-Everhelm Teflon-glass homogenizer. The mixture was then centrifuged at 14,000 × *g* for 10 min at 4 °C, and 50 μl of the supernatant was supplemented with 2.5 μl of a mixture of internal standards containing 0.1 nmol/μl of d_3-acetylcarnitine + 0.02 nmol/μl of d_3-propionylcarnitine + 0.02 nmol/μl of d_3-butyrylcarnitine + 0.02 nmol/μl of d_3-octanoylcarnitine + 0.04 nmol/μl of d_3-palmitoylcarnitine. Acylcarnitine esters were extracted (22, 23) and measured by direct injection electrospray tandem mass spectrometry using a Quattro Micro LC-MS system (Waters-Micromass, Milford, MA) equipped with a model HTS-PAL autosampler (Leap Technologies, Carrboro, NC), a model 1100 high pressure liquid chromatography solvent delivery system (Agilent Technologies), and a data system running MassLynx software.

Histology—Mouse tissues were fixed in 4% phosphate-buffered paraformaldehyde (pH 7.4), embedded in paraffin, sectioned (5 μm), and stained with hematoxylin and eosin.

Quantitative Reverse Transcriptase PCR-based Gene Expression Analysis—RNA was isolated from frozen liver samples using a commercially available kit (Qiagen RNeasy kit, Qiagen Inc., Valencia, CA) in combination with DNase digest treatment. Then 1.5 μg of total RNA was reverse transcribed (Stratagene, La Jolla, CA) with random oligo primers. PCR was performed with a DNA Engine Opticon 2 System (MJ Research, Boston, MA) using the SYBR Green QPCR dye kit (Stratagene, La Jolla, CA). Long-chain acyl-CoA dehydrogenase, FAS, SREBP1c, PPARγ, PPARα, glucose-6-phosphatase, and 18 S rRNA were amplified using this system. Product specificity was verified by running products on an agarose gel. Reactions were performed in duplicate and messenger RNA levels (ΔC_T values) normalized to 18 S rRNA were expressed using the comparative method. 18 S rRNA levels showed no statistical difference between groups.

Quantitative reverse transcriptase-PCR for peroxisome proliferator-activated receptor-γ coactivator-1α, mitochondrial HMG-CoA synthase, CPT1, PEPCK, mtGPAT1, ACO, and SCD1 was performed using an ABI PRISM 7000 Sequence Detection System instrument and TaqMan® Universal PCR Master Mix used according to the manufacturer's specifications (Applied Biosystems, Inc., Foster City, CA). Reactions were performed in triplicate and contained 20 ng of cDNA as template, 900 nM forward and reverse primers, and 200 nM probe. Target gene expression was normalized to 18 S rRNA levels, which were assayed by multiplexing with the manufacturer's 5′ VIC-labeled, primer-limited 18 S endogenous control premix. Primers and 5′ FAM-labeled TaqMan probes were purchased as pre-validated assays (ABI) or designed using Primer Express® software and sequences available in GenBank™. Relative quantification of target genes was calculated using the $2^{-\Delta\Delta C_T}$ method (24), which was validated for each primer/probe set using a 6-point serial standard curve as described previously (25). Derivation of the $2^{-\Delta\Delta C_T}$ equation has been described in Applied Biosystems User Bulletin No. 2 (P/N 4303859).

Statistics—Data were analyzed by Student's *t* test or by analysis of variance (ANOVA). ANOVA was performed on data at a minimum $p < 0.05$ threshold and a multiple comparison Fischer post-hoc test was performed to evaluate differences between genotypes and dietary treatments with JMP software version 5 (SAS Institute Inc., Cary, NC). Data are shown as mean ± S.E.

RESULTS

The High Fat/High Sucrose Diet Increased Weight Gain and Plasma Lipids—To induce lipogenesis, 2-month-old male mtGPAT1 +/+ (wild type), +/− (heterozygote), and −/− (deficient) mice were fed either a high fat/high sucrose or a low fat/low sucrose control diet for 4 months. Body weights increased 80% on the HH diet and 30% on the LL diet, as did all measured fat pad weights (Fig. 1). When expressed as a percent of total body weight, isolated gonadal and retroperitoneal fat pads were 2.5-fold greater, and brown adipose tissue was 1.4-fold greater in mice fed the HH diet. Adipose tissue histology revealed larger adipocytes from gonadal tissue in mice fed the HH diet than in mice fed the LL diet (Fig. 2, *C* and *D*). Correlating with the development of obesity in mice fed the HH diet, the plasma leptin concentrations were 5-fold higher, and, similar to changes previously reported on this diet (12), plasma concen-

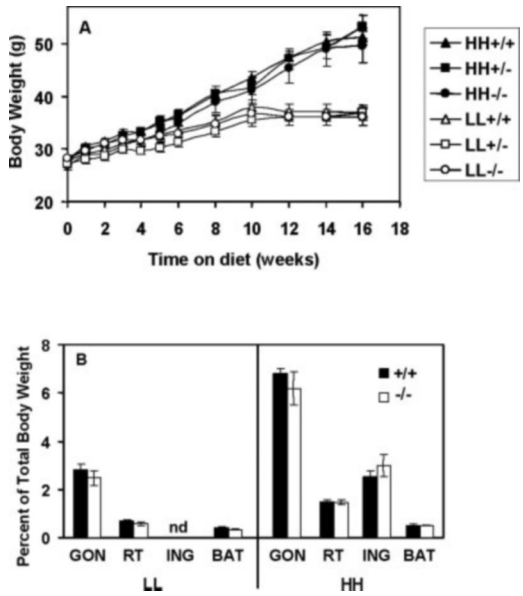

FIG. 1. **mtGPAT1$^{-/-}$ mice are not resistant to diet-induced obesity.** *A*, weight gain of male mice on LL (+/+, $n = 11$; +/−, $n = 12$; −/−, $n = 10$) and HH (+/+, $n = 13$; +/−, $n = 11$; −, $n = 9$) diets fed from 2 to 6 months of age. *B*, fat pad weights as percent of total body weight of male mice after 4 months on LL (+/+, $n = 11$; −/−, $n = 10$) diet and on HH (+/+, $n = 7$; −/−, $n = 6$) diets. Gonadal (*GON*), retroperitoneal (*RT*), inguinal (*ING*), brown adipose tissue (*BAT*) are indicated. *ND*, not determined

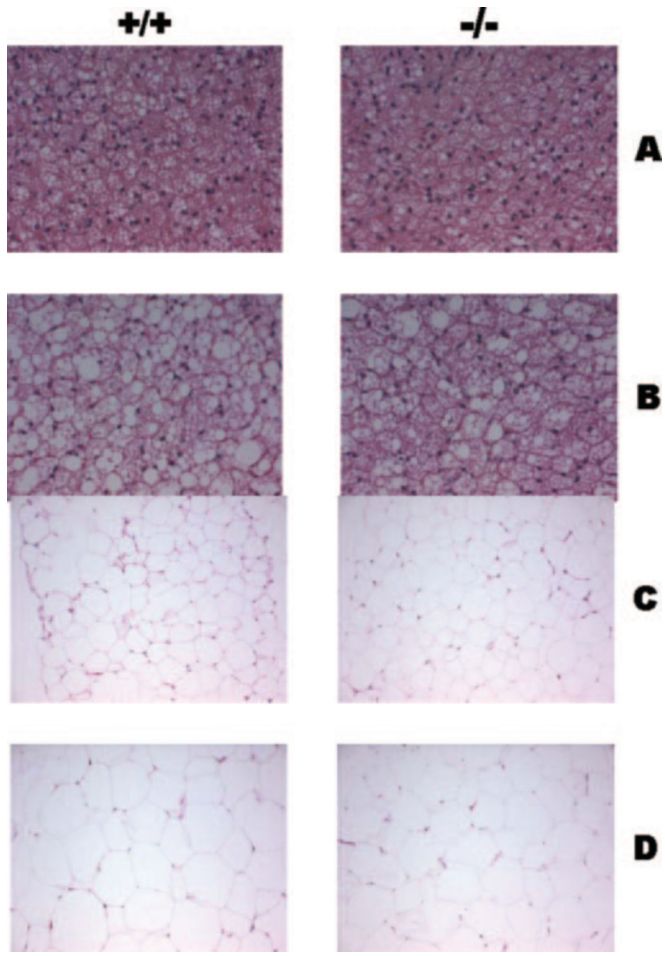

FIG. 2. **HH feeding increases lipid accumulation in adipose tissue.** Morphology of interscapular brown adipose tissue from mtGPAT1$^{-/-}$ and wild type mice fed (*A*) LL and (*B*) HH diets for 4 months. Morphology of gonadal fat from mtGPAT1$^{-/-}$ and wild type mice fed (*C*) LL or (*D*) HH diets for 4 months. Paraffin sections are stained with hematoxylin and eosin.

trations of triacylglycerol, cholesterol, free fatty acid, glucose, and insulin were elevated (Table I).

mtGPAT1$^{-/-}$ Mice Were Not Resistant to Diet-induced Obesity—Despite the marked effect that the HH diet had on weight gain and fat pad weight, there were no differences in terminal body weight or individual fat pad weight by genotype (Fig. 1), and the weights of liver, kidney, and skeletal (soleus and extensor digitorum longus) muscle did not differ between genotypes on either diet (data not shown). The lack of difference between genotypes in percent of lean and fat body mass was confirmed by densitometry (PIXImus, Faxitron X-ray Corporation) (data not shown). Adipocyte size was similar between genotypes in both LL and HH fed mice (Fig. 2, *A–D*). Consistent with the lack of difference in fat pad weights, the plasma leptin concentrations did not differ between genotypes (Table I).

mtGPAT1$^{-/-}$ Mice Accumulate Less Hepatic Triacylglycerol and Lysophosphatidic Acid—In vitro and animal studies show a direct correlation between increased mtGPAT1 activity and triacylglycerol accumulation in liver (13, 26), as well as hyperlipidemia in mice fed the HH diet (12). Thus, we expected that absent mtGPAT1 would result in lower liver triacylglycerol content and lower plasma lipids. Although plasma triacylglycerol values did not differ between genotypes fed the HH diet, cholesterol concentrations were 20% lower in the mtGPAT1$^{-/-}$ mice (Table I).

Hepatocytes from mtGPAT1$^{-/-}$ mice fed the HH diet contained smaller lipid vacuoles than the corresponding wild type controls, and triacylglycerol content in mtGPAT1$^{-/-}$ liver was 60% lower on the HH diet and 40% lower on the LL diet (Fig. 3). As expected, lysophosphatidic acid, the product of mtGPAT1, was 50% lower in mtGPAT1$^{-/-}$ mice (Fig. 4), and the C16:0, C16:1, and C18:1-lysophosphatidic acid species were decreased most strongly in mtGPAT1$^{-/-}$ mice compared with wild type controls on both diets (data not shown). Thus, in liver from mtGPAT1$^{-/-}$ mice, less acyl-CoA is channeled toward triacylglycerol synthesis.

Ketogenesis Is Increased in mtGPAT1$^{-/-}$ Mice—A consequence of reduced partitioning of fatty acid into triacylglycerol synthesis could be increased oxidation and ketogenesis, the latter directly correlated with β-oxidation. With the LL diet, no difference in plasma β-hydroxybutyrate values was observed between wild type and mtGPAT1$^{-/-}$ mice. With the HH diet, however, β-hydroxybutyrate increased in both genotypes, and was 2-fold higher in the mtGPAT1$^{-/-}$ mice than in the wild type controls (Table I). In the mtGPAT1$^{-/-}$ mice, the increase in β-hydroxybutyrate was associated with a 2-fold increase in the expression of HMG-CoA synthase, the rate-limiting enzyme in ketogenesis (Table II). Expression of PPARα, and its mitochondrial targets CPT1 and long-chain acyl-CoA dehydrogenase did not differ between genotypes on either diet, although there was a diet-induced increase in peroxisomal acyl-CoA oxidase. Thus, the robust changes in acyl-CoA partitioning were not associated with a global induction of PPARα-targeted genes.

Hepatic Acyl-CoA Content Is Increased in mtGPAT1$^{-/-}$ Mice—If the absence of mtGPAT1 allows more acyl-CoA to enter the pathways of β-oxidation and ketogenesis, one might expect to find lower plasma-free fatty acid and hepatic acyl-CoA concentrations relative to wild type controls. As predicted, plasma-free fatty acid in mtGPAT1$^{-/-}$ mice fed the HH diet was about 10% lower (Table I). Unexpectedly, however, the liver content of acyl-CoA in mtGPAT1$^{-/-}$ mice fed either diet was 3-fold higher than in wild type controls (Fig. 5*A*), and the most prevalent liver acyl-CoA species, 16:0, 16:1,

TABLE I
Plasma values for mtGPAT1$^{-/-}$ and wild-type mice fed HH or LL diets

Numbers of samples analyzed for each measurement are in parentheses. Values are presented as mean ± S.E, analyzed by Student *t*-test. Values with different superscript numbers differ significantly; p value < 0.05.

	LL		HH		p value[a]	
Genotype	+/+	−/−	+/+	−/−	Geno-type	diet
Leptin (ng/ml)	5.8 ± 1.1[1] (10)	5.8 ± 1[1] (8)	28.0 ± 2.1[2] (10)	27.5 ± 3.1[2] (7)	NS	0.001
Triacylglycerol (mg/dl)	39 ± 2[1] (10)	35 ± 3[1] (10)	44 ± 4[2,3] (13)	43 ± 2[2,3] (8)	NS	<0.05
Cholesterol (mg/dl)	80 ± 7[1] (9)	76 ± 5[1] (9)	166 ± 5[2] (13)	133 ± 8[3] (8)	0.02	0.0001
FFA (mM)	0.41 ± 0.06[1,2] (10)	0.36 ± 0.04[1,3] (9)	0.59 ± 0.06[4] (9)	0.53 ± 0.07[2,3,4] (8)	0.04	0.03
β-Hydroxybutyrate (μM)	138 ± 43[1] (5)	233 ± 59[1] (5)	386 ± 37[2] (9)	777 ± 112[3] (10)	0.003	<0.0001
Glucose (mg/dl)	127 ± 8[1] (10)	130 ± 6[1] (13)	174 ± 18[2] (7)	193 ± 10[2] (9)	NS	<0.001
Insulin (ng/dl)	0.62 ± 0.18[1] (10)	0.55 ± 0.18[1] (13)	1.09 ± 0.22[2] (7)	1.87 ± 0.24[3] (9)	0.03	<0.008
IR index[b]	3.8 ± 0.9[1] (10)	2.8 ± 0.4[1] (13)	10.1 ± 2.6[2] (7)	17.2 ± 3.6[2] (9)	NS	0.0001

[a] Calculated by ANOVA; NS, no statistically significant difference.
[b] IR index (insulin resistance index) was calculated as the product of the areas under the glucose and insulin curves as described under "Materials and Methods."

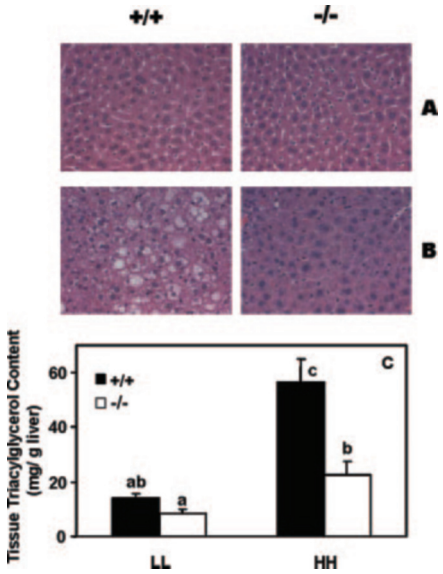

FIG. 3. **mtGPAT1$^{-/-}$ mice accumulate less hepatic triacylglycerol.** Representative liver paraffin sections stained with hematoxylin and eosin at 6 months from mtGPAT1$^{-/-}$ and wild type mice fed (*A*) LL and (*B*) HH diets for 4 months. *C*, liver triacylglycerol content from mice fed LL (+/+, $n = 5$; −/−, $n = 4$) or HH (+/+, $n = 6$; −/−, $n = 5$) diets. Data are shown are mean ± S.E.; *columns* identified with different letters differ significantly (p value < 0.05, *ANOVA*).

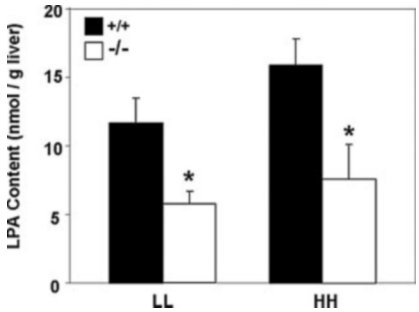

FIG. 4. **Liver lysophosphatidic acid is low in mtGPAT1$^{-/-}$ mice.** Total liver acyl-CoA values at 6 months from mtGPAT1$^{-/-}$ and wild type mice fed LL (+/+, $n = 5$; −/−, $n = 4$) and HH diets (+/+, $n = 6$; −/−, $n = 5$) for 4 months. Data shown are mean ± S.E. *, p value < 0.05 compared with wild type by Student's *t* test.

18:0, 18:1, and 18:2, were 2.5–6-fold more abundant in the mtGPAT1$^{-/-}$ mice (Fig. 5, *B* and *C*). This distribution of acyl-CoAs differed from the fatty acid composition of both diets (Fig. 4, *D* and *E*), but the predominant acyl-CoA species were similar to the long-chain fatty acid composition of the

TABLE II
Gene expression in liver from mtGPAT1$^{-/-}$ and WT mice fed HH and LL diets

Total RNA was extracted from liver of wild type (+/+) and GPAT null (−/−) mice fed on a HH or LL diet ($n = 5$ for HH +/+, $n = 6$ for all other groups). Gene expression levels were determined by real-time quantitative PCR as described under "Materials and Methods" and are presented as –fold change (mean ± S.E.) relative to the LL +/+ controls. Results were analyzed by ANOVA and Student's *t* test. Significant differences (p value < 0.05) between groups are indicated by dissimilar superscript numbers.

	LL		HH	
Genotype	+/+	−/−	+/+	−/−
mtGPAT1	1.0 ± 0.15[1]	ND[1]	1.89 ± 0.26[2]	ND
mtHS2[b]	1.0 ± 0.18[1]	1.0 ± 0.08[1]	0.88 ± 0.22[1]	1.74 ± 0.15[2]
CPT1	1.0 ± 0.20	0.75 ± 0.12	1.03 ± 0.18	0.75 ± 0.07
LCAD	1.0 ± 0.38	0.91 ± 0.23	0.99 ± 0.18	1.21 ± 0.13
ACO	1.0 ± 0.18[1]	0.87 ± 0.09[1]	2.49 ± 0.39[2]	1.81 ± 0.19[2]
PPARα	1.0 ± 0.25	0.63 ± 0.05	0.95 ± 0.13	0.81 ± 0.14
PGC-1α	1.0 ± 0.09	1.39 ± 0.29	1.28 ± 0.24	0.94 ± 0.21
PPARγ	1.0 ± 0.29[1]	1.22 ± 0.43[1,2]	2.18 ± 0.44[2,3]	1.97 ± 0.46[2,3]
SREBP1c	1.0 ± 0.16	1.39 ± 0.45	1.17 ± 0.30	1.43 ± 0.27
FAS	1.0 ± 0.28	1.04 ± 0.25	1.26 ± 0.57	1.86 ± 0.92
SCD1	1.0 ± 0.27[1]	1.23 ± 0.26[1]	0.95 ± 0.19[1]	0.44 ± 0.07[2]
G6P	1.0 ± 0.18[1]	1.33 ± 0.32[1]	0.35 ± 0.12[2]	0.80 ± 0.17[1,2]
PEPCK	1.0 ± 0.09	1.14 ± 0.05	0.90 ± 0.15	0.84 ± 0.23

[a] ND, not determined.
[b] The abbreviations used in the table are: mitochondrial 3-hydroxy-3-methylglutaryl-CoA synthase (mtHS2), acyl-CoA oxidase (ACO), carnitine palmitoyltransferase-1 (CPT1), long-chain acyl-CoA dehydrogenase (LCAD), PPAR α and γ, peroxisome proliferator-activated receptor-γ coactivator-1α (PGC-1α), PEPCK, SREBP1c, FAS, SCD1, glucose-6-phosphatase (G6P).

diet. To ascertain whether the long-chain acyl-CoAs might originate in the diet or from newly synthesized fatty acid, we examined the expression of SREBP-1c and its target gene, fatty acid synthase; neither differed between genotypes (Table II). The lack of increase in FAS mRNA expression in the mtGPAT1$^{-/-}$ mice suggests that the pathway of *de novo* fatty acid synthesis was not up-regulated. Because medium-chain fatty acids are preferentially oxidized, the accumulation of long-chain acyl-CoAs in mtGPAT1$^{-/-}$ mouse liver reflects the inability of the mitochondria to handle excess fatty acids when mtGPAT1 is not available to divert them toward glycerolipid synthesis. Interestingly, although 18:1-CoA was the most abundant acyl-CoA identified on both the HH and LL diets, the expression of stearoyl-CoA desaturase (SCD), the enzyme that forms oleoyl-CoA, was decreased 50% in the HH fed mtGPAT1$^{-/-}$ mice (Table II), suggesting that an elevation in oleoyl-CoA might down-regulate SCD-1.

Diet, fatty acid, and acyl-CoAs regulate gene transcription controlled by SREBP, HNF4α, and PPAR-α and -γ (27). Compared with mice fed the LL diet, mice fed the HH diet showed

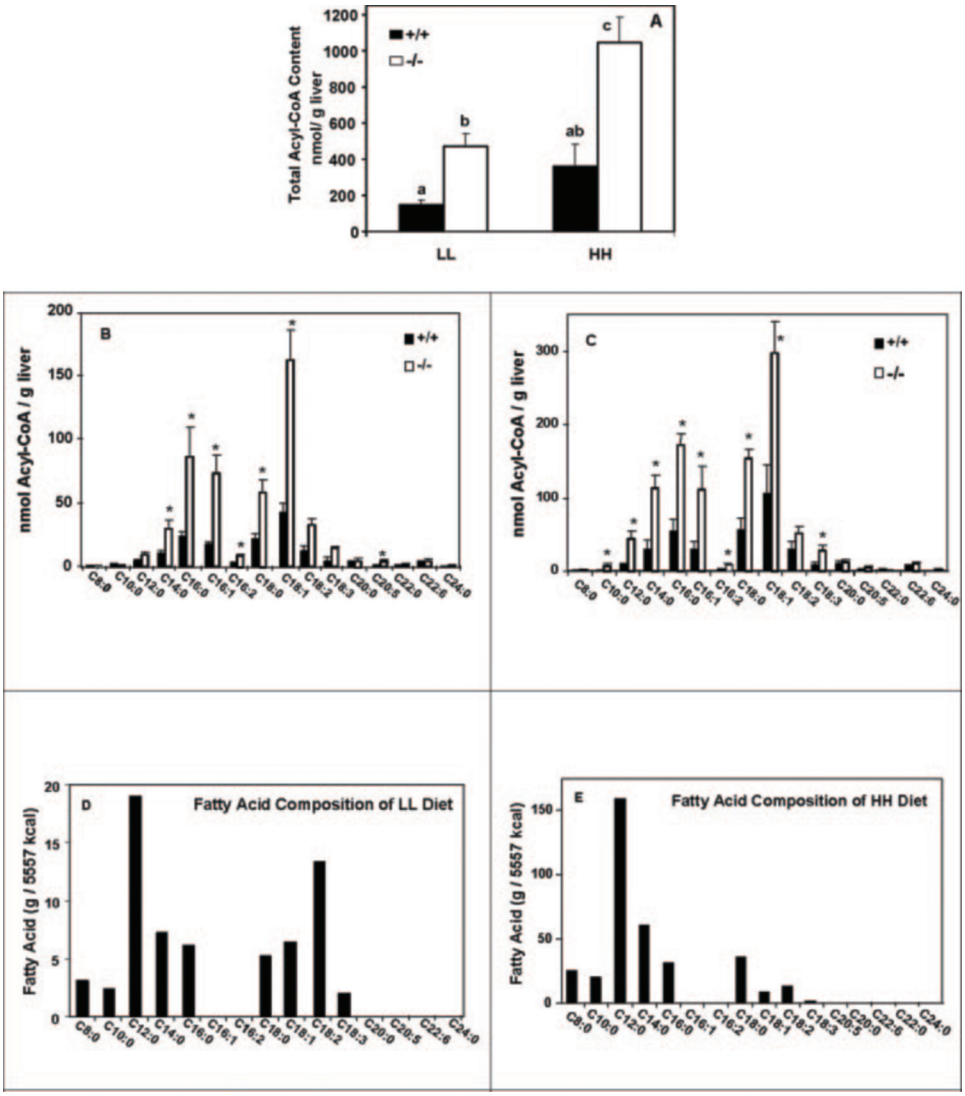

FIG. 5. **Liver acyl-CoA content is elevated in mtGPAT1$^{-/-}$ mice.** *A*, total liver acyl-CoA values from mtGPAT1$^{-/-}$ and wild type mice fed LL (+/+, $n = 5$; −/−, $n = 4$) and HH diets (+/+, $n = 6$; −/−, $n = 5$) for 4 months. *B* and *C*, liver acyl-CoA composition of mice fed the LL diet (+/+, $n = 5$; −/−, $n = 4$) (*B*) or the HH diet (+/+, $n = 6$; −/−, $n = 5$) for 4 months (*C*). *D*, fatty acid composition of LL diet: Research Diets D12328. *E*, fatty acid composition of HH diet: Research Diets D12331. Data are shown as mean ± S.E.; *columns* identified with different letters or the *asterisk* (*) differ significantly (p value < 0.05, Student's t test).

an increase in hepatic expression of PPARγ, which is up-regulated in liver by high fat feeding (28), but no change in PPARα, SREBP1c, or peroxisome proliferator-activated receptor-γ coactivator-1α (Table II). The expression of these transcription factors did not differ between genotypes.

Hepatic Acylcarnitines Increase in mtGPAT1$^{-/-}$ Mice—To gain a more comprehensive analysis of hepatic fatty acid catabolism we profiled mitochondrial-derived acylcarnitine esters. These analytes reflect mitochondrial accumulation of fatty acyl-CoAs and dicarboxylic acids and thus provide information regarding substrate flux through specific steps of the β-oxidation spiral. In both control and mtGPAT1$^{-/-}$ mice, the HH diet increased hepatic accumulation of medium-chain (C6, C8, and C10) acylcarnitine derivatives (Fig. 6, *A* and *B*), consistent with high mitochondrial uptake and catabolism of medium-chain fatty acids. The HH diet also increased hepatic levels of β-OH-butyrylcarnitine, a marker of accelerated β-oxidation and ketogenesis. Whereas most medium-chain metabolites were unaffected by genotype, diet-induced accumulation of the dicarboxylic analyte, C8-DC, the long-chain acylcarnitines (C16, C18, C18:1, and C18:2), and the long-chain hydroxy-acylcarnitines (C16-OH, C18-OH, and C18:1-OH) were greater in liver from the mtGPAT1$^{-/-}$ mice compared with control mice.

High Fat Feeding Induces Changes in Insulin Responsiveness in mtGPAT1$^{-/-}$ Mice—The HH diet resulted in higher fasting plasma glucose and insulin in both genotypes (Table I). Plasma insulin values were 70% higher in the mtGPAT1$^{-/-}$ mice compared with wild type mice (Table I), suggesting an increase in insulin resistance. To determine the response of the mtGPAT1$^{-/-}$ and wild type mice to a glucose load, a glucose tolerance test was performed. The rates of glucose and insulin clearance after a glucose load did not differ between genotypes that had been fed the LL diet (Fig. 7, *A* and *C*). In contrast to the LL diet, the HH fed mice developed fasting hyperglycemia accompanied by pronounced hyperinsulinemia and a reduced glucose tolerance with a slower rate of glucose clearance for mtGPAT1$^{-/-}$ mice (Fig. 7, *B* and *D*). Plasma insulin values tended to be higher in mtGPAT1$^{-/-}$ mice, but were not significantly different from wild type animals. Although the calculated insulin resistance index was 2.7- and 6.1-fold higher, respectively, in both genotypes fed the HH compared with the LL diet, it did not differ significantly by genotype (Table I). Despite glucose intolerance at a whole-body level, the HH diet

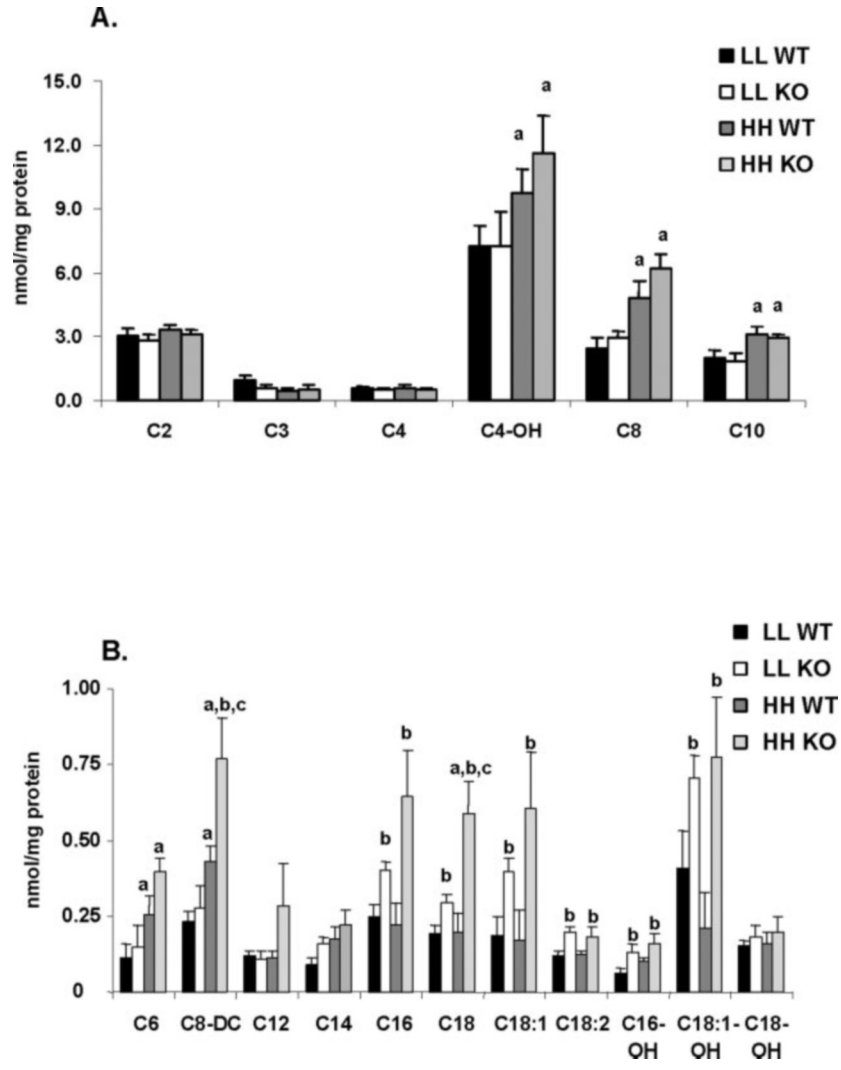

FIG. 6. **Long-chain acylcarnitines are high in mtGPAT1$^{-/-}$ mice.** Hepatic acylcarnitine values from mtGPAT1$^{-/-}$ and wild type mice fed LL (+/+, $n = 5$; −/−, $n = 4$) and HH diets (+/+, $n = 6$; −/−, $n = 5$) for 4 months. *A*, major acylcarnitine species; *B*, minor acylcarnitine species. The data are shown as mean ± S.E. Significant differences are indicated by (*a*) for diet, (*b*) for genotype, and (*c*) for an interaction between diet and genotype (p value < 0.05, *ANOVA*). *OH*-, hydroxyl; *DC*, dicarboxylic. *WT*, wild type; *KO*, knock-out.

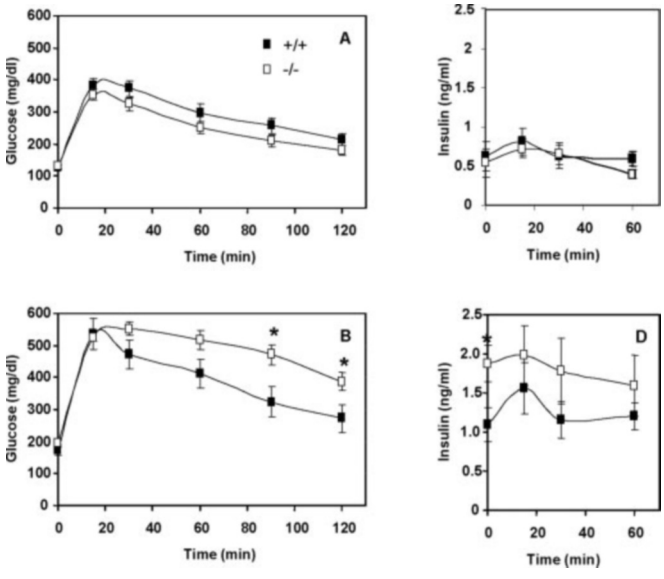

FIG. 7. **mtGPAT1$^{-/-}$ mice have reduced glucose tolerance with HH feeding.** *A*, plasma glucose concentrations during an intraperitoneal glucose tolerance test on male and female mice fed the LL diet (+/+, $n = 10$; −/−, $n = 13$); or *B*, the HH diet (+/+, $n = 7$; −/−, $n = 9$) for 4 months. *C*, plasma insulin concentrations during an intraperitoneal glucose tolerance on male and female mice fed the LL diet (+/+, $n = 10$; −/−, $n = 13$); or *D*, the HH diet (+/+, $n = 7$; −/−, $n = 9$) for 4 months. Data shown are mean ± S.E.; values identified by (*) differ significantly (p value < 0.05, Student's t test).

still suppressed glucose-6-phosphatase, but not PEPCK, in wild type controls (Table II). In contrast, the mtGPAT1$^{-/-}$ mice failed to down-regulate glucose-6-phosphatase in response to the HH diet, suggesting that hepatic insulin resistance was more severe when mtGPAT1 was absent (Table II).

DISCUSSION

Obesity and dysregulation of lipid metabolism is associated with hepatic steatosis and hyperlipidemia (29). mtGPAT1, which catalyzes the initial step in triacylglycerol synthesis, is a key regulator of triacylglycerol metabolism in liver (2), where it comprises 30–50% of total GPAT activity (2). The expression of mtGPAT1 is regulated both nutritionally and hormonally in a manner consistent with a prominent role in triacylglycerol synthesis (30). For example, mtGPAT1 mRNA expression increases 19-fold 6 h after insulin is given to streptozotocin-diabetic mice, and 20-fold when food restricted mice are refed a high-carbohydrate, fat-free diet (4). The up-regulation by insulin is mediated by SREBP-1c, which also acts to increase the expression of lipogenic target genes like acetyl-CoA carboxylase and FAS (31, 32).

Because they are intrinsic proteins of the outer mitochondrial membrane, it has been hypothesized that mtGPAT1 and CPT1 control the partitioning of acyl-CoAs between incorporation into glycerolipid synthesis and β-oxidation. mtGPAT1 and carnitine palmitoyltransferase-1 are reciprocally regulated by AMPK that phosphorylates and inhibits acetyl-CoA carboxylase, thereby decreasing the malonyl-CoA-mediated allosteric

inhibition of carnitine palmitoyltransferase-1 (10). AMPK also inhibits mtGPAT1 activity, decreasing the incorporation of labeled [^{14}C]oleate and [^{3}H]glycerol incorporation into triacylglycerol and increasing labeled [^{14}C]oleate incorporation into acid soluble metabolites (9). Overexpressing rat mtGPAT1 in Chinese hamster ovary and HEK293 cells increases triacylglycerol mass and the incorporation of labeled [^{14}C]oleate into triacylglycerol (26). In rat hepatocytes, adenoviral-mediated overexpression of mouse or rat mtGPAT1 decreases labeled [^{14}C]oleate incorporation into oxidation pathways and increases [^{14}C]oleate incorporation into triacylglycerol (13, 14).

Because these *in vitro* studies suggest that mtGPAT1 partitions acyl-CoAs toward synthetic and away from degradative pathways, we examined the physiological consequences of absent mtGPAT1 on acyl-CoA partitioning. mtGPAT1$^{-/-}$ mice were fed a high fat/high sucrose diet to promote the development of hepatic lipogenesis, triacylglycerol synthesis, and obesity (12, 15, 17, 33). A previous study showed that when mice were fed a high fat (lard)/high sucrose diet for 3 months, hepatic mtGPAT1 mRNA increased 2-fold (13), and the present study shows a similar increase of mtGPAT1 expression in wild type controls. As expected, the absence of mtGPAT1 protected against hepatic steatosis. Our data show that mtGPAT1$^{-/-}$ mice fed the HH diet had 60% lower hepatic triacylglycerol content and increased ketogenesis compared with wild type controls.

Ketogenesis is regulated at three steps: 1) provision of fatty acids from adipose tissue lipolysis and/or dietary sources; 2) the CPT1-mediated synthesis of long-chain acylcarnitines for entry into the mitochondria (or the direct entry of dietary medium-chain fatty acids); and 3) the activity of mitochondrial HMG-CoA synthase, which catalyzes the irreversible initial step in ketogenesis (34). In mtGPAT1$^{-/-}$ mice fed the HH diet, the 2-fold increase in plasma β-hydroxybutyrate coincided with a 2-fold increase in the expression of mitochondrial HMG-CoA synthase, suggesting that metabolic changes resulting from the absence of mtGPAT1 are able to up-regulate HMG-CoA synthase without altering PPARα or its other mitochondrial target genes, CPT1 and long-chain acyl-CoA dehydrogenase.

The lack of difference in SREBP1c and FAS expression related to either diet or genotype suggests that the increase in acyl-CoA content did not result from increased *de novo* synthesis but, rather, to an inability to use excess acyl-CoAs derived from dietary fatty acids. Medium-chain fatty acids are preferentially oxidized without conversion to acylcarnitines (35), whereas the 16- and 18-carbon fatty acids in the HH diet require CPT1 to convert their acyl-CoA derivatives to acylcarnitines. The preferred substrate of mtGPAT1 is 16:0-CoA, which is esterified at rates 3–10-fold higher than those for other long-chain acyl-CoAs (36–39). Although some elongation of medium-chain fatty acids may occur (40), our study strongly suggests that the normal metabolism of long-chain acyl-CoAs, even when derived from the LL diet that contains only 10.5% triacylglycerol, requires the ability of mtGPAT1 to acylate glycerol 3-phosphate. Long-chain acyl-CoAs accumulated when the synthetic pathway was absent because the amount of acyl-CoA exceeded the capacity of the mitochondrial oxidation pathway. Thus, it appears that mtGPAT1 is required to channel excess long-chain acyl-CoAs toward triacylglycerol synthesis.

In contrast to the medium-chain metabolites, long-chain acylcarnitines were unchanged by the HH diet, but increased in the mtGPAT null genotype. Similar to the acyl-CoA profile, hepatic concentrations of most long-chain acylcarnitines were highest in the mtGPAT1$^{-/-}$ mice fed the HH diet. Thus, as predicted, deletion of mtGPAT1 appears to increase CPT1-mediated transport of long-chain acyl-CoAs into the mitochondria. Notably, hepatic content of the long-chain hydroxyl-acylcarnitines (*e.g.* C18:1-OH) was greater in mtGPAT1$^{-/-}$ mice compared with wild type mice. Accumulation of these metabolites, which is thought to reflect a flux limitation at the hydroxyacyl-CoA dehydrogenase step, suggests that the long-chain acyl-CoA supply exceeded the β-oxidative capacity of liver mitochondria. In the aggregate, our results imply that the mtGPAT1 null condition increases mitochondrial uptake of long-chain fatty acyl-CoAs via elevated CPT1 activity and/or increased substrate supply. The excessive β-oxidative pressure, in turn, elicited a compensatory induction of mitochondrial 3-hydroxy-3-methylglutaryl-CoA synthase and a concomitant rise in hepatic ketogenesis.

Although oleoyl-CoA (18:1-CoA) was the most abundant acyl-CoA that accumulated, the expression of SCD-1, the enzyme that catalyzes the *de novo* synthesis of 18:1-CoA was 50% lower in the livers from the HH fed mtGPAT1$^{-/-}$ mice. SCD-1 transcription is repressed by linoleic acid, arachidonic acid, and eicosapentaenoic acid (41), and transcription of SCD-1 is regulated by SREBP1c (42). *In vitro* studies have demonstrated that 18:1 and polyunsaturated fatty acids inhibit SREBP-mediated transcription and decrease the processing of mature SREBP proteins (43, 44). Thus, the 3-fold elevation in 18:1-CoA levels in the liver of the HH fed mtGPAT1$^{-/-}$ mice may have down-regulated SCD-1 via SREBP1c. However, the lack of change in FAS, which is also a target of SREBP1c, suggests that additional factors may contribute to the specificity of the fatty acid-mediated effect on SCD1. Alternatively, discordant effects may result from functionally different metabolic pools of 18:1, one derived from the diet and the other from *de novo* synthesis (42).

Similar to a previous report of the HH diet effects on wild type mice (12), both HH fed mtGPAT1$^{-/-}$ and wild type mice became hyperglycemic and hyperinsulinemic. It has been proposed that reduced insulin sensitivity is related to an increase in intracellular lipid metabolites of triacylglycerol in liver and peripheral tissues (45) and that, in muscle, elevated intracellular lipid metabolites such as diacylglycerol or acyl-CoAs induce insulin resistance by activating PKCθ, which initiates a serine/threonine kinase cascade that increases serine/threonine phosphorylation and decreases tyrosine phosphorylation of IRS1/IRS2. The aberrant phosphorylation results in lower phosphatidylinositol 3-kinase activity, and ultimately diminishes insulin sensitivity (45). In liver from rats fed a high fat (safflower oil) diet for 3 days, alterations in the insulin signaling cascade associated with hepatic insulin resistance include decreased IRS1 and IRS2 phosphotyrosine, decreased IRS1- and IRS2-phosphatidylinositol 3-kinase activity, decreased AKT2 and GSK3 activity, and decreased glycogen synthase activity (46). In these high fat-fed rats, liver acyl-CoAs and triacylglycerol content are about 3-fold higher and the suppression of endogenous glucose production is diminished compared with rats fed a control diet (46). In contrast, the mtGPAT1$^{-/-}$ mice fed the HH diet for 4 months in our study had a lower hepatic triacylglycerol content but higher liver acyl-CoA levels, higher plasma insulin concentrations, and diminished glucose tolerance. The differences and commonalities between the 3-day safflower oil diet and the 4-month HH diet suggest that causative factors of reduced insulin sensitivity may include a complex association between the dietary source of fatty acid, the length of exposure, and the lipid metabolite accumulation.

Hepatic acyl-CoA levels in mtGPAT1$^{-/-}$ mice fed the LL or HH diet were about 3-fold higher than in wild type mice, but PEPCK and glucose-6-phosphatase mRNA was not suppressed by the HH diet, suggesting the presence of hepatic insulin resistance. Glucose intolerance in the mtGPAT1$^{-/-}$ mice fed

the HH diet may also be caused by diminished glucose uptake in peripheral tissues. Because hepatic acyl-CoAs were elevated while liver triacylglycerol content remained low in the mtGPAT1$^{-/-}$ mice, further studies will be needed to determine whether this discordant relationship alters the response of the liver to insulin.

The major effects of mtGPAT1 deficiency are observed in liver where this GPAT isoform contributes 50% of total activity; in contrast, the mtGPAT1 isoform comprises only 10% of total GPAT activity in adipose tissue (30). In our previous study of mice fed a low fat chow, the body weight at 5 months and fat pad weights at 12 months were lower in female, but not male mtGPAT1$^{-/-}$ mice (7). The present study again shows similar body and fat pad weights of male mtGPAT1$^{-/-}$ and wild type mice, suggesting that the mtGPAT1 isoform may not play an important role in controlling triacylglycerol storage in fat cells in male mice.

In the present study we have examined the physiological consequences of high fat/high sucrose feeding on the hepatic partitioning of acyl-CoAs in mice that lack mtGPAT1. Increased partitioning of acyl-CoAs toward ketogenesis was demonstrated by increased plasma β-hydroxybutyrate and increased expression of mtHMG-CoA synthase. In addition, we found diminished partitioning of acyl-CoAs toward synthetic pathways demonstrated by reduced hepatic triacylglycerol content and an elevated content of long-chain acyl-CoAs. The hepatic acyl-CoAs may have contributed to the repression of lipogenic gene expression and the induction of ketogenesis. This study demonstrates the crucial role that mtGPAT1 plays in controlling the partitioning acyl-CoAs between oxidative and synthetic pathways and in diverting excess fatty acids toward triacylglycerol synthesis, even when the diet contains relatively little triacylglycerol.

REFERENCES

1. Browning, J. D., and Horton, J. D. (2004) *J. Clin. Investig.* **114,** 147–152
2. Bell, R. M., and Coleman, R. A. (1983) in *The Enzymes* (Boyer, P. D., ed) Vol. XVI, pp. 87–112, Academic Press, New York
3. Lewin, T. M., Schwerbrock, N. M. J., Lee, D. P., and Coleman, R. A. (2004) *J. Biol. Chem.* **279,** 13488–13495
4. Shin, D.-H., Paulauskis, J. D., Moustaid, N., and Sul, H. S. (1991) *J. Biol. Chem.* **266,** 23834–23839
5. Yet, S.-F., Lee, S., Hahm, Y. T., and Sul, H. S. (1993) *Biochemistry* **32,** 9486–9491
6. Lewin, T. M., Granger, D. A., Kim, J.-H., and Coleman, R. A. (2001) *Arch. Biochem. Biophys.* **396,** 119–127
7. Hammond, L. E., Gallagher, P. A., Wang, S., Posey-Marcos, E., Hiller, S., Kluckman, K., Maeda, N., and Coleman, R. A. (2002) *Mol. Cell. Biol.* **22,** 8204–8214
8. Hardie, D. G., Corton, J., Ching, Y. P., Davies, S. P., and Hawley, S. (1997) *Biochem. Soc. Trans.* **25,** 1226–1228
9. Muoio, D. M., Seefield, K., Witters, L., and Coleman, R. A. (1999) *Biochem. J.* **338,** 783–791
10. Coleman, R. A., Lewin, T. M., and Muoio, D. M. (2000) *Annu. Rev. Nutr.* **20,** 77–103
11. Park, H., Kaushik, V. K., Constant, S., Prentki, M., Przybytkowski, E., Ruderman, N. B., and Saha, A. K. (2002) *J. Biol. Chem.* **277,** 32571–33257
12. Surwit, R. S., Feinglos, M. N., Rodin, J., Sutherland, A., Petro, A. E., Opara, E. C., Kuhn, C. M., and Rebuffe-Scrive, M. (1995) *Metab. Clin. Exp.* **44,** 645–651
13. Lindén, D., William-Olsson, L., Rhedin, M., Asztély, A.-K., Clapham, J. C., and Schreyer, S. (2004) *J. Lipid Res.* **45,** 1279–1288
14. Lewin, T. M., Wang, S., Nagle, C. A., Van Horn, C. G., and Coleman, R. A. (2004) *Am. J. Physiol.* **288,** E835–E844
15. Collins, S., Daniel, K. W., Petro, A. E., and Surwit, R. S. (1997) *Endocrinology* **128,** 405–413
16. Collins, S., Martin, T. L., Surwit, R. S., and Robidoux, J. (2004) *Physiol. Behav.* **81,** 243–248
17. Black, B. L., Croom, J., Eisen, E. J., Petro, A. E., Edwards, C. L., and Surwit, R. S. (1998) *Metabolism* **47,** 1354–1359
18. Zammit, V. A., Waterman, I. J., Topping, D., and McKay, G. (2001) *J. Nutr.* **131,** 2074–2077
19. Yamauchi, T., Kamon, J., Waki, H., Terauchi, Y., Kubota, N., Hara, K., Mori, Y., Ide, T., Murakami, K., Tsuboyama-Kasaoka, N., Ezaki, O., Akanuma, Y., Gavrilova, O., Vinson, C., Reitman, M. L., Kagechika, H., Shudo, K., Yoda, M., Nakano, Y., Tobe, K., Nagai, R., Kimura, S., Tomita, M., Froguel, P., and Kadowaki, T. (2001) *Nature Med.* **7,** 941–946
20. Folch, J., Lees, M., and Stanley, G. H. S. (1957) *J. Biol. Chem.* **226,** 497–509
21. Deutsch, J., Grange, E., Rapoport, S. I., and Purdon, A. D. (1994) *Anal. Biochem.* **220,** 321–323
22. Millington, D. S., Kodo, N., Norwood, D. L., and Roe, C. R. (1990) *J. Inherit. Metab. Dis.* **13,** 321–324
23. An, J., Muoio, D. M., Shiota, M., Fujimoto, Y., Cline, G. W., Shulman, G. I., Koves, T. R., Stevens, R., Millington, D. S., and Newgard, C. B. (2004) *Nat. Med.* **10,** 268–274
24. Livak, K. J., and Schmittgen, T. D. (2001) *Methods* **25,** 402–408
25. Muoio, D. M., MacLean, P. S., Lang, D. B., Li, S., Houmard, J. A., Way, J. M., Winegar, D. A., Corton, J. C., Dohm, G. L., and Kraus, W. E. (2002) *J. Biol. Chem.* **277,** 26089–26097
26. Igal, R. A., Wang, S., Gonzalez-Baró, M., and Coleman, R. A. (2001) *J. Biol. Chem.* **276,** 42205–42212
27. Jump, D. B. (2002) *Curr. Opin. Lipidol.* **13,** 155–164
28. Vidal-Puig, A., Jimenez-Linan, M., Lowell, B. B., Hamann, A., Hu, E., Spiegelman, B., Flier, J. S., and Moller, D. E. (1996) *J. Clin. Investig.* **97,** 2553–2561
29. Thuresson, E. R. (2004) *Curr. Opin. Investig. Drugs* **5,** 411–418
30. Coleman, R. A., and Lee, D. P. (2004) *Prog. Lipid Res.* **43,** 134–176
31. Horton, J. D., Goldstein, J. L., and Brown, M. S. (2002) *J. Clin. Investig.* **109,** 1125–1131
32. Horton, J. D. (2002) *Biochem. Soc. Trans.* **30,** 1091–1095
33. Black, P. N., and DiRusso, C. C. (1994) *Biochim. Biophys. Acta* **1210,** 123–145
34. Fukao, T., Lopaschuk, G. D., and Mitchell, G. A. (2004) *Prostaglandins Leukotrienes Essent. Fatty Acids* **70,** 243–251
35. Bonnefont, J. P., Demaugre, F., Prip-Buus, C., Saudubray, J. M., Brivet, M., Abadi, N., and Thuillier, L. (1999) *Mol. Genet. Metab.* **68,** 424–440
36. Monroy, G., Kelker, H. C., and Pullman, M. E. (1973) *J. Biol. Chem.* **248,** 2845–2852
37. Bremer, J., Bjerve, K. S., Borrebaek, B., and Christiansen, R. (1976) *Mol. Cell Biochem.* **12,** 113–125
38. Kelker, H. C., and Pullman, M. E. (1979) *J. Biol. Chem.* **254,** 5364–5371
39. Yet, S.-F., Moon, Y. K., and Sul, H. S. (1995) *Biochemistry* **34,** 7303–7310
40. Stein, T. P., Presti, M. E., Leskiw, M. J., Torosian, M. E., Settle, R. G., Buzby, G. P., and Schluter, M. D. (1984) *Am. J. Physiol.* **246,** E277–E287
41. Waters, K. M., Miller, C. W., and Ntambi, J. M. (1997) *Biochim. Biophys. Acta* **1349,** 33–42
42. Ntambi, J. M., and Miyazaki, M. (2004) *Prog. Lipid Res.* **43,** 91–104
43. Thewke, D. P., Panini, S. R., and Sinensky, M. (1998) *J. Biol. Chem.* **273,** 21402–21407
44. Worgall, T. S., Sturley, S. L., Seo, T., Osborne, T. F., and Deckelbaum, R. J. (1998) *J. Biol. Chem.* **273,** 25537–25540
45. Shulman, G. I. (2000) *J. Clin. Investig.* **106,** 171–176
46. Samuel, V. T., Liu, Z. X., Qu, X., Elder, B. D., Bilz, S., Befroy, D., Romanelli, A. J., and Shulman, G. I. (2004) *J. Biol. Chem.* **279,** 32345–32353